

# Analysis of Jitter in Phase-Locked Loops

David C. Lee, *Senior Member, IEEE*

**Abstract**—Jitter in clock signals is analyzed, linking noise in free-running oscillators to short-term and long-term time-domain behavior of phase-locked loops. Particular attention is given to comparing the impact of  $1/f$  noise and white noise in oscillators and frequency dividers on jitter in phase-locked loops of first- and second-order. Theoretical analysis is supported by results obtained using mixed-signal behavior simulation.

**Index Terms**— $1/f$  noise, frequency dividers, jitter, oscillators, phase noise, phase-locked loops (PLLs), white noise.

## I. INTRODUCTION

**I**N A free-running oscillator that is perturbed by white noise such as thermal noise, transition times are known to follow a random-walk process, such that the variance of period jitter grows linearly with the measurement interval [1]–[3]. When this oscillator is used in a first-order phase-locked loop (PLL), the variance of period jitter rises at the same linear rate, and saturates exponentially for measurement intervals longer than the reciprocal of the loop bandwidth [4]. The literature on PLL noise is extensive. However, until very recently [5], little is known about this measurement-interval dependence for a second-order system. While some progress has been made in understanding how flicker noise affects phase noise in an oscillator (for example, making transition waveforms more symmetric reduces  $1/f$  noise upconversion [6]), it remains unclear if and how period jitter can be predicted in practice. A frequency divider can add significant noise with white and  $1/f$  spectrum [7]–[10]. Flicker noise affects jitter in a PLL in several intriguing ways, but this topic is rarely discussed, with one notable exception [11]. It is worthwhile to note that ring-oscillator simulation in [12] indicates that supply and substrate noise is the main source of jitter, while recent PLL measurement and analysis in [13] demonstrates that PLL jitter strongly depends on the power-supply distribution network. More specifically, when the power supply configuration is designed to minimize the impact of supply and substrate noise, device noise can be the dominant cause of PLL jitter.

The organization of the paper is as follows. In Section II, three time-domain measures of clock jitter are defined. The general link between time-domain results and frequency-domain results is established. This section provides further motivations for this work, and lays the foundation for the remainder of the paper.

Manuscript received April 24, 2002; revised October 23, 2002. This paper was recommended by Associate Editor K. Yang.

The author was with Mentor Graphics Corporation, Allentown, PA 18103 USA. He is now with BDA, Allentown PA 18103 USA (e-mail: davidlee@ieee.org).

Digital Object Identifier 10.1109/TCSII.2002.807265

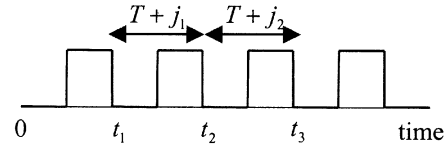


Fig. 1. Clock signal with transition-time jitter.

In Section III, the timing property of free-running oscillators, in the presence of white and  $1/f$  noise, is presented. Contrary to [6], the variance of period jitter is not well defined for oscillators with significant  $1/f$  noise, because it fails to converge for large sample sizes. An alternate measure of jitter, introduced in Section II, is free of this limitation. In Section IV, phase noise analysis of linear(ized) PLLs is discussed. Jitter in PLLs of first- and second-order is systematically analyzed in Sections V and VI. In many applications, the dominant cause of jitter is usually white and  $1/f$  noise in voltage-controlled oscillators (VCO). The link from VCO noise to PLL jitter is established here. In Section VII, techniques for achieving fast and timing-accurate mixed-signal jitter simulation are discussed. Simulation result for a 2.56 GHz charge-pump PLL is compared with theoretical prediction. Flicker noise in frequency dividers has a peculiar effect on the behavior of PLLs. Analysis and simulation, presented in Section VIII, reveal that the tracking error between the PLL output and the reference oscillator grows with time and is potentially unbounded.

## II. ABSOLUTE JITTER, PERIOD JITTER AND ADJACENT PERIOD JITTER

Suppose  $\{t_n\}$  is a sequence of transition times from a clock with nominal period  $T$  (Fig. 1). The sequence

$$\{t_n - nT\} \quad (1)$$

characterizes **absolute jitter**. This is also known as aperture jitter or aperture uncertainty, which limits the resolution of Analog-to-Digital converters [14]. Absolute jitter in radian,<sup>1</sup> with respect to nominal frequency  $f_0 = 1/T$ , is given by

$$\{\theta_n := 2\pi f_0(t_n - nT)\}. \quad (2)$$

It is well-known that the variance for stationary absolute jitter is related to the total area of its power spectrum

$$\sigma_A^2 = \frac{1}{(2\pi f_0)^2} \int_{-f_0/2}^{f_0/2} S_\theta(f) df. \quad (3)$$

<sup>1</sup>In this paper,  $\theta$  denotes absolute jitter, and is distinct from phase noise  $\phi$  that will be introduced later in Section III.

Here,  $S_\theta(f)$  denotes the spectral density<sup>2</sup> (in rad<sup>2</sup>/Hz) of  $\theta$ . Absolute jitter is also used to describe the tracking error between two clocks (for example, VCO and reference oscillator in a PLL).

Intuitively, the sequence

$$\{j_n := t_{n+1} - t_n - T\} \quad (4)$$

characterizes the variation in the period from the nominal period. Commonly known as **period jitter**, it reduces the time available for data processing per clock cycle, and limits the clock frequency at which a digital system can run without short-cycle failures. This is also called cycle jitter in [12], edge-to-edge jitter, and cycle-to-cycle jitter in [1] and [2]. Jitter over  $k$  periods can be measured using

$$\{j_n(kT) := t_{n+k} - t_n - kT\}. \quad (5)$$

This is sometimes referred as long-term jitter. In a graphics card, long-term jitter in the pixel clock is kept to a minimum in order to achieve a sharp display.

The second difference of absolute jitter provides another measure of jitter known as **adjacent period jitter** (APJ)

$$\{\Delta j_n := j_{n+1} - j_n = (t_{n+2} - t_{n+1}) - (t_{n+1} - t_n)\}. \quad (6)$$

This characterizes the local change in the period, from one cycle to an adjacent cycle. Excessive adjacent-period jitter causes large-displacement failures and undermines the reliability of clock distribution systems with multiple synchronous clocks (PLLs). Confusingly, this is also called cycle-to-cycle jitter in [12]. In this paper, the author calls (1) and (2) absolute jitter, (4) and (5) period jitter, and (6) and (7) adjacent period jitter. More generally, the sequence

$$\{\Delta j_n(kT) := t_{n+2k} - 2t_{n+k} + t_n\} \quad (7)$$

measures the “local” change in jitter over  $k$  periods.

Period jitter and adjacent period jitter are time-domain concepts, and their variances can be calculated directly from time-interval measurements. These quantities can also be determined from the spectral density of absolute jitter. The variance for (stationary) period jitter is obtained by integrating the power spectrum of  $\{j_n(kT)\}$

$$\sigma_{j_n}^2(kT) = \frac{1}{(\pi f_0)^2} \int_{-f_0/2}^{f_0/2} \sin^2(\pi f kT) S_\theta(f) df. \quad (8)$$

This result can be derived as follows. The period jitter sequence is the first difference of the absolute jitter sequence. In  $z$ -domain, this operation is  $D(z) := 1 - z^{-k}$ . The above is obtained by premultiplying  $S_\theta(f)$  in (3) by

$$\begin{aligned} |D(\omega)|^2 &= D(z)D(z^{-1})\Big|_{z=e^{j\omega}} = 2 - 2\cos(k\omega) \\ &= \left\{2\sin\left(\frac{k\omega}{2}\right)\right\}^2. \end{aligned}$$

<sup>2</sup>Power spectral density of a wide-sense stationary process is formally defined as the Fourier transform of the autocorrelation function. For many processes considered in this work, the Fourier transform does not exist. In this paper, the terms “spectral density” and “power spectrum” refer to the spectrum obtained using a periodogram.

Similarly, the variance for (stationary) adjacent period jitter is obtained by integrating the power spectrum of  $\{\Delta j_n(kT)\}$

$$\sigma_{\Delta J}^2(kT) = \frac{4}{(\pi f_0)^2} \int_{-f_0/2}^{f_0/2} \sin^4(\pi f kT) S_\theta(f) df. \quad (9)$$

As stated earlier, the adjacent-period jitter sequence is the second difference of the absolute jitter sequence, and this operation is  $D^2(z) := (1 - z^{-k})^2$ . Premultiplying  $S_\theta(f)$  in (3) by

$$|D^2(\omega)|^2 = |D(\omega)|^4 = \{2 - 2\cos(k\omega)\}^2 = \left\{2\sin\left(\frac{k\omega}{2}\right)\right\}^4$$

results in (9). In (8) and (9), notice that deterministic or random frequency components near integer multiples of  $1/kT$  do not contribute to (adjacent) period jitter measured over  $k$  periods. As a direct consequence of the spectrum given in (8) and (9), there is a simple, not previously known, relation between period jitter and adjacent period jitter

$$\sigma_{\Delta J}^2(kT) = 4\sigma_J^2(kT) - \sigma_J^2(2kT). \quad (10)$$

This relation can be verified by noting the algebraic identity:  $\{2 - 2\cos(k\omega)\}^2 = 4\{2 - 2\cos(k\omega)\} - \{2 - 2\cos(2k\omega)\}$ . Additionally, the three measures of jitter have these properties

$$\begin{aligned} \frac{\sigma_J(kT)}{\sigma_A} &\leq 2, & \frac{\sigma_{\Delta J}(kT)}{\sigma_A} &\leq 4, \\ \frac{\sigma_{\Delta J}(kT)}{\sigma_J(kT)} &\leq 2 \\ \frac{\sigma_J(2kT)}{\sigma_J(kT)} &\leq 2. \end{aligned} \quad (11a-d)$$

The first two properties are due to the fact that the integral in (3) is larger than the integrals in (8) and (9). The next two properties hold because variances are nonnegative, and the rightmost (leftmost) term in (10) has a lower bound of zero. These general results will be used to analyze short-term and long-term time-domain behavior of oscillators and phase-locked loops.

In the above, (3), (8), and (9), with integration limits  $\pm f_0/2$ , are appropriate for the absolute jitter sequence  $\{\theta_n\}$ . From an analysis point of view, it is sometimes useful to treat absolute jitter  $\theta(s)$  as a continuous function of the absolute clock phase  $s$  in time unit, such that  $\{\theta(nT)\} = \{\theta_n\}$ . It is well-known that (3), with integration limits replaced by  $\pm\infty$ , is appropriate for  $\theta(s)$ . Since the delay operation for a continuous signal and a discrete sequence has the same Fourier transform, the same (8) and (9), with integration limits replaced by  $\pm\infty$ , are appropriate for  $\theta(s)$ . The expression for period jitter variance  $\sigma_J^2(T)$  is similar to the one in [6], and is simpler than the one in [15]. It should be noted  $\sigma_{\Delta J}^2(kT)/2(kT)^2$  is the Allan variance commonly used in stability analysis of precision clocks and oscillators [16].

### III. JITTER AND PHASE NOISE IN FREE-RUNNING OSCILLATORS

A simple model of a free-running oscillator with amplitude  $A$ , nominal frequency  $f_0$ , and phase noise  $\phi(t)$  is

$$v(t) = A \sin(2\pi f_0 t + \phi(t)) \quad (12)$$

with instantaneous frequency  $f_0 + (d\phi(t)/dt)/2\pi$ . Higher order harmonics and amplitude noise are assumed negligible. Phase noise is typically characterized using the two-sided spectral density of  $\phi(t)$ ,  $S\phi(f)$  in  $\text{rad}^2/\text{Hz}$ , or the single-sideband spectrum (in  $1/\text{Hz}$ )

$$\mathcal{L}(f_m) := 4Sv(f_0 + f_m)/A^2 \quad (13)$$

where  $Sv(f)$  is the two-sided spectral density of the oscillator waveform. A typical phase-noise spectrum is of the form

$$S\phi(f) = f_0^2 (c f^{-2} + c_{\text{FN}}|f|^{-3}). \quad (14)$$

The  $c$  term is white frequency noise, and the  $c_{\text{FN}}$  term is flicker frequency noise. It is common to assume that the  $\mathcal{L}(f_m)$  spectrum has the same form when the offset frequency is not too small.

In the above model of an oscillator,  $\phi(t)$  is phase noise. Phase noise causes absolute jitter  $\{\theta_n\}$  [or  $\theta(s)$ ,  $s = t + \phi(t)/2\pi f_0$ ] that is defined in Section II. A clock that is running faster than normal has a positive  $\phi(t)$ . As transitions are arriving earlier,  $\{\theta_n\}$  is negative. Because  $\{\theta_n\}$  and  $\phi(t)$  characterize different aspects of a process, they can have different statistical properties. In the following analysis, it is assumed that absolute jitter  $\theta(s)$  has the same power spectrum as phase noise  $\phi(t)$ , i.e.

$$S_\theta(f) \approx S\phi(f), \quad -\infty < f < +\infty. \quad (15)$$

This is supported by the following observations. In a free-running oscillator that is perturbed by white noise,  $\phi(t)$  follows a Wiener process (Brownian motion) [1], [2], and  $kT$ -increments of  $s(t) := t + \phi(t)/2\pi f_0$  are Gaussian with mean  $kT$  and variance  $c kT$ . Consequently, first-crossing times in  $s(t)$  follow a random-walk process, and the length of  $k$  oscillation periods has the asymmetric inverse Gaussian distribution with identical mean  $kT$  and variance  $c kT$  [3]. Equation (15) is justified since the pair has the same second-order statistics. It is not known whether a similar property holds for flicker frequency noise.

Using (9), the variance for adjacent period jitter is given by [16]

$$\sigma_{\Delta J}^2(kT) = 2c|kT| + 8\ln(2)c_{\text{FN}}(kT)^2. \quad (16)$$

The slope in a log-log plot of  $\sigma_{\Delta J}^2(kT)$  steepens at  $0.36(c_{\text{FN}}/c)^{-1}$ , where  $c_{\text{FN}}/c$  is the  $1/f^3$  corner frequency in the  $S\phi(f)$  spectrum. This suggests an alternate method of obtaining  $c$  and  $c_{\text{FN}}$  in (14) from time-interval-analyzer measurement. Notice that the rate of change in the period has a standard deviation,  $\sigma_{\Delta J}(kT)/kT$ , that is bounded.

Using (8), the period jitter variance due to white frequency noise is given by [1], [2]

$$\sigma_J^2(kT) = c|kT|. \quad (17)$$

As noted earlier, this result can be derived directly [3] without using (15). For a single period, the rms period jitter is

$$\sigma_J(T) = \sqrt{cT} = \kappa \sqrt{T} \quad (18)$$

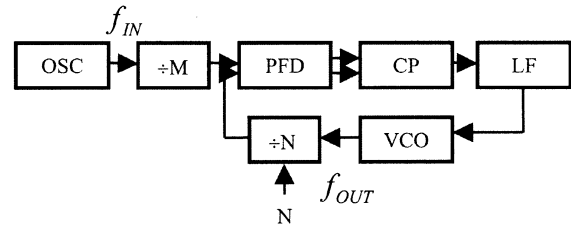


Fig. 2. Charge-pump PLL.

where  $c$  is the parameter defined by Demir *et al.* [2], and  $\kappa$  is defined by McNeill [4]. This can also be determined from phase-noise measurement

$$\sigma_J(T) \approx \sqrt{\mathcal{L}(f_m) f_m^2 / f_0^3} \quad (19)$$

where  $10 \log_{10} \mathcal{L}(f_m)$  falls at the rate of 20 dBc/Hz per decade. Notice that  $\sigma_{\Delta J}(T) = \sqrt{2} \sigma_J(T)$  [12]. However, the period jitter variance due to  $1/f^3$  phase noise is potentially unbounded. This result, while unsettling, should be expected. The period jitter sequence is  $1/f$  noise produced by the first difference of  $1/f^3$  noise. It is well-known that  $1/f$  noise has infinite memory (long-term correlation), and infinite variance in the sense that the variance is an increasing function of the sequence length. For this reason, the use of adjacent period jitter is preferred. In [6], ring-oscillator data suggests that rms period jitter is proportional to  $kT$ , but no analytical method is provided for calculating the proportionality constant. As a practical matter, obtaining a meaningful value for period jitter (for a free-running oscillator) is not as important as understanding how  $1/f$  noise in the oscillator affects the overall period jitter in a PLL. The latter is discussed in detail in Sections V and VI.

Using (3), the absolute jitter variance  $\sigma_A^2$  is infinite. In a free-running oscillator,  $\phi(t)$  and  $\theta(s)$  drift without bound, and have infinite power.

#### IV. PLL PHASE NOISE

Fig. 2 shows a typical charge-pump phase-locked loop (PLL). It consists of reference oscillator with input frequency  $f_{\text{IN}}$ , voltage-controlled oscillator (VCO) with output frequency  $f_{\text{OUT}}$ , frequency dividers (FD), phase/frequency detector (PFD), charge pump (CP) and loop filter (LF). Using negative feedback, the VCO phase is adjusted to track the reference oscillator phase so that the skew between the two PFD inputs is constant. At steady state, this achieves (in a time-averaged sense) the desired synchronization function

$$\frac{f_{\text{OUT}}}{N} = \frac{f_{\text{IN}}}{M} \quad (20)$$

where  $N$  and  $M$  are digitally programmable divider ratios. Deterministic and random disturbance present in the various circuit blocks causes jitter and phase noise in the overall system.

Assuming the sampling rate of the PFD exceeds 10 times the loop bandwidth, a classic continuous-time model of the PLL can be derived by linearizing around the steady state expressed by (20). This is shown in Fig. 3. Here,  $\phi$  denotes the excess phase in radian relative to a carrier frequency signal,  $K_{\text{PD}} = I_{\text{CP}}/2\pi$ ,  $K_{\text{VCO}} = 2\pi G_{\text{VCO}}$ ,  $F(s)$  is the loop filter,  $I_{\text{CP}}$  is the

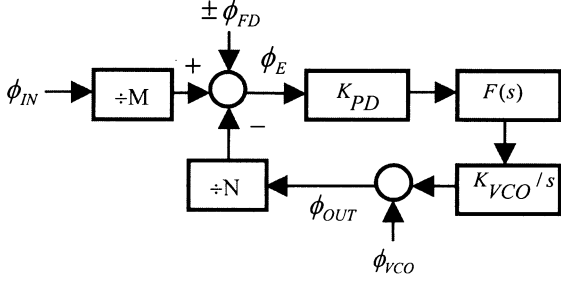


Fig. 3. Linear continuous-time PLL model.

charge-pump current, and  $G_{VCO}$  is the small-signal VCO gain in Hz/volt. The output phase noise is usually due to phase noise in the VCO and the reference input. Simple analysis shows that the transfer function from input to output is

$$\frac{\phi_{OUT}}{\phi_{IN}} = \frac{K_{PD}K_{VCO}F(s)/M}{s + K_{PD}K_{VCO}F(s)/N} = \frac{N}{M} H(s) \quad (21)$$

and the transfer function from VCO to output is

$$\frac{\phi_{OUT}}{\phi_{VCO}} = \frac{s}{s + K_{PD}K_{VCO}F(s)/N} = 1 - H(s). \quad (22)$$

In general,  $H(s)$  is a low-pass filter that suppresses input noise outside the loop bandwidth.  $1 - H(s)$  is a high-pass filter that suppresses VCO noise within the loop bandwidth by the loop gain. In other words, increasing the loop bandwidth reduces the effect of cumulative VCO jitter, while decreasing it reduces the influence of input jitter. Suppose noise sources in the reference input and the VCO are uncorrelated. Denoting their respective phase-noise spectra by  $S\phi_{REF}(f)$  and  $S\phi_{VCO}(f)$ , the PLL output spectrum is given by

$$S\phi_{OUT}(f) = \{N/M\}^2 |H(f)|^2 S\phi_{REF}(f) + |1 - H(f)|^2 S\phi_{VCO}(f). \quad (23)$$

This result can be generalized to include noise sources in the frequency dividers, the phase/frequency detector, the charge pump and the loop filter; as well as correlated noise sources such as supply and substrate noise. An excellent discussion on the effect of supply and substrate noise on PLL jitter, caused by digital switching circuits, is given in [13]. In the following sections, the effect of VCO noise on the time-domain behavior of PLLs is analyzed using the above results in conjunction with those given in Section II. It is reasonable to expect that the PLL behaves like the reference oscillator over long measurement intervals, and like the (free-running) VCO over short measurement intervals, such that time-domain results for oscillators (given in Section III) can provide useful approximations and insights.

In [17], the  $\mathcal{L}(f_m)$  spectrum at the PLL output is calculated from the solution to a stochastic differential equation that is derived from a linear continuous-time model of the PLL. This novel method is useful when an accurate  $\mathcal{L}(f_m)$  spectrum is desired, but has the limitation that  $1/f$  noise cannot be handled. The focus of the present work is jitter and the effect of white and  $1/f$  noise on jitter, which is directly related to  $S_\phi(f)$  or  $S_\theta(f)$ . It should be noted that  $S_\theta(f)$  in the equations given in Section II cannot be replaced by  $\mathcal{L}(f_m)$ .

## V. JITTER IN FIRST-ORDER PLL

A first-order PLL of loop bandwidth  $\omega_L/2\pi$  has

$$H(s) = \frac{\omega_L}{s + \omega_L}. \quad (24)$$

With white frequency noise in the VCO, the output spectrum is flat up to the loop bandwidth. Using the results of Section IV and (3), (8)–(10) of Section II, the output jitter statistics are given by

$$\begin{aligned} \sigma_A^2 &= \frac{c}{2\omega_L} \\ \sigma_J^2(kT) &= 2\sigma_A^2 \left\{ 1 - e^{-\omega_L|kT|} \right\} \\ \sigma_{\Delta J}^2(kT) &= 6\sigma_A^2 \left\{ 1 - \frac{4}{3} e^{-\omega_L|kT|} + \frac{1}{3} e^{-2\omega_L|kT|} \right\}. \end{aligned} \quad (25)$$

As expected, widening PLL bandwidth and reducing VCO jitter minimizes absolute jitter. The first two expressions are identical to those in [4]. The third expression is not previously known, and can be derived using (9) or (10). Comparing the Maclaurin series expansion of the latter two expressions with (16) and (17), it is evident that over measurement intervals shorter than  $1/\omega_L$ , the PLL behaves like a free-running VCO. Reducing cumulative VCO jitter minimizes short-term (adjacent) period jitter. Over measurement intervals longer than  $1/\omega_L$ , (adjacent) period jitter variance becomes constant. In general, one would expect that as  $k \rightarrow \infty$ ,  $\sigma_J^2(kT) \rightarrow 2\sigma_A^2$  (as noted by McNeill in [4]) and  $\sigma_{\Delta J}^2(kT) \rightarrow 6\sigma_A^2$  [due to (10)], though exceptions exist. In this paper, the author calls  $\sigma_J^2(kT)/2\sigma_A^2$  the normalized period-jitter variance, and  $\sigma_{\Delta J}^2(kT)/6\sigma_A^2$  the normalized adjacent-period-jitter variance. Normalized variances are bounded by  $\sigma_J^2(kT)/2\sigma_A^2 \leq 2$  and  $\sigma_{\Delta J}^2(kT)/6\sigma_A^2 \leq 2(2/3)$ , because of (11a–b).

With  $1/f^3$  phase noise in the VCO, the output spectrum has  $1/f$  dependence below the loop bandwidth. Because of divergence in (3), the absolute jitter variance is potentially unbounded. Fortunately, practical PLLs are typically second-order systems such that  $|1 - H(f)|$  rolls off more rapidly toward the origin.

## VI. JITTER IN SECOND-ORDER PLL

A second-order (Type II) PLL has

$$H(s) = \frac{2\zeta\omega_n s + \omega_n^2}{s^2 + 2\zeta\omega_n s + \omega_n^2} \quad (26)$$

where  $\omega_n$  is the natural frequency and  $\zeta$  is the damping factor. Like the previous section, expressions for absolute jitter, period jitter, and adjacent period jitter can be derived using the results of Sections II and IV. With white and flicker frequency noise in the VCO, the absolute jitter variance at the PLL output is

$$\sigma_A^2 = \frac{c}{4\zeta\omega_n} + \frac{c_{FN}}{\omega_n^2} f(\zeta) \quad (27)$$

where

$$\begin{aligned} f(\zeta) &= \frac{\pi/2 - \arctan(\zeta/\sqrt{1-\zeta^2})}{\zeta\sqrt{1-\zeta^2}}, & \zeta < 1 \\ &= \frac{\Re\left\{\operatorname{arctanh}\left(\zeta/\sqrt{\zeta^2-1}\right)\right\}}{\zeta\sqrt{\zeta^2-1}}, & \zeta > 1 \end{aligned}$$

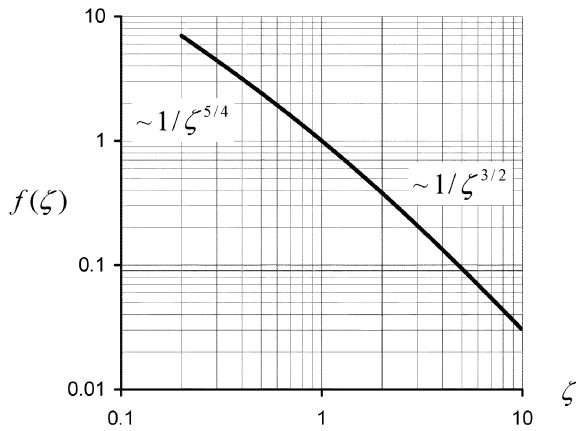


Fig. 4. Graph of  $f(\zeta)$  for  $0.2 < \zeta < 10$ .

is the monotonic, decreasing function shown in Fig. 4. A similar plot appears in [11, p 105] and in [18]. Taking the ratio of the second term to the first term, the relative contribution of  $1/f$  noise to absolute jitter variance is proportional to the ratio of the  $1/f^3$  corner frequency in  $S\phi_{VCO}(f)$  to the natural frequency of the PLL

$$4f(\zeta)\zeta \frac{c_{FN}/c}{\omega_n} \approx \frac{0.64}{\sqrt{\zeta}} \frac{c_{FN}/c}{\omega_n/2\pi}. \quad (28)$$

In the above expression, the author approximates  $f(\zeta)$  by  $1/\zeta^{3/2}$  over the range:  $1 < \zeta < 10$ . In [18],  $f(\zeta)$  is approximated by  $2.5/\zeta^2$  for  $4 < \zeta < 20$ . It can be verified numerically that  $f(\zeta) \approx 1/\zeta^{3/2}$  is more accurate over the range  $1 < \zeta < 20$ , and is exact at  $\zeta = 1$ .

A PLL with maximally flat  $|H(f)|$  response is often desired, and this is obtained with  $\zeta = 1/\sqrt{2}$ . With white frequency noise in the VCO, the output jitter statistics are given by

$$\begin{aligned} \sigma_A^2 &= \frac{\sqrt{2}c}{4\omega_n} \\ \sigma_J^2(kT) &= 2\sigma_A^2 h(\omega_n |kT|) \end{aligned} \quad (29)$$

where  $(\tau := |kT|)$

$$h(\omega_n\tau) := 1 - \sqrt{2} \exp\left(-\frac{\omega_n\tau}{\sqrt{2}}\right) \cos\left(\frac{\pi}{4} + \frac{\omega_n\tau}{\sqrt{2}}\right).$$

It can be shown that the slope of  $\sigma_J^2(kT)$  in (29), for small  $kT$ , is identical to that of (17) for a free-running VCO. Very recently, general analytical expressions of  $\sigma_J^2(kT)$  for  $\zeta < 1$  and  $\zeta > 1$  have been reported in [5]. With  $1/f^3$  phase noise in the VCO, the output jitter statistics are given by

$$\begin{aligned} \sigma_A^2 &= \frac{\pi c_{FN}}{2\omega_n^2} \\ \sigma_J^2(kT) &= 2\sigma_A^2 h_{FN}(\omega_n |kT|). \end{aligned} \quad (30)$$

Figs. 5 and 6 show graphs of the normalized period-jitter variance  $h(\omega_n\tau)$  and  $h_{FN}(\omega_n\tau)$  respectively, indicating that period jitter over some measurement intervals can exceed its long-term value by 20%. Plots similar to Fig. 5 can also be found in [5]. The normalized APJ variances are shown in Figs. 7 and 8, and can be obtained using (9) or (10). These analytical results are

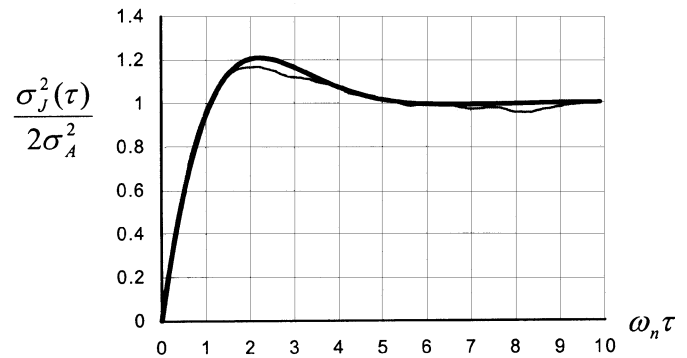


Fig. 5. Normalized period-jitter variance caused by white frequency noise: theory (thick line) versus simulation (thin line).

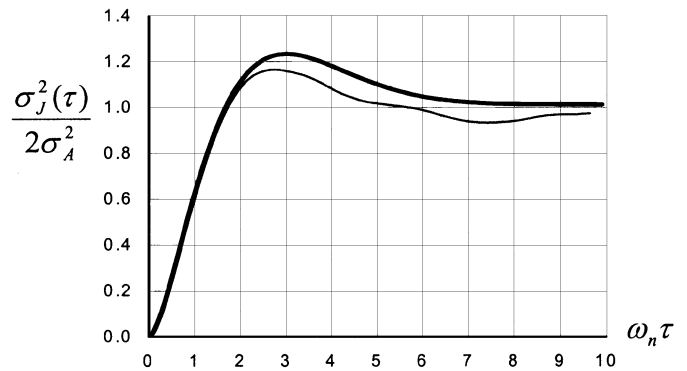


Fig. 6. Normalized period-jitter variance caused by flicker frequency noise: theory (thick line) versus simulation (thin line).

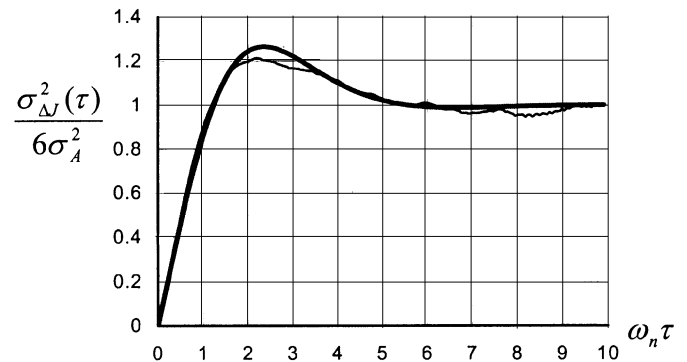


Fig. 7. Normalized adjacent-period-jitter variance caused by white frequency noise: theory (thick line) versus simulation (thin line).

validated using mixed-signal jitter simulation that is described in the next section. Note that normalized APJ (Figs. 7 and 8) can be at most 33% higher than normalized period jitter (Figs. 5 and 6), due to the bound given in (11c).

To examine the short-term behavior of the PLL, the four normalized variances are graphed on a log-log plot in Fig. 9 to show  $\omega_n\tau$  dependence over measurement intervals shorter than  $1/\omega_n$ . With white frequency noise in the VCO,  $\sigma_J^2(\tau)$  and  $\sigma_{AJ}^2(\tau)$  (upper curves in Fig. 9) are linear in the measurement interval. With flicker frequency noise,  $\sigma_{AJ}^2(\tau)$  (bottom curve) is quadratic in the measurement interval. Thus far, the time-domain behavior is consistent with that of a free-running VCO, as expressed by (16) and (17). Fig. 9 reveals that with flicker frequency noise in the VCO, the dependence of period jitter

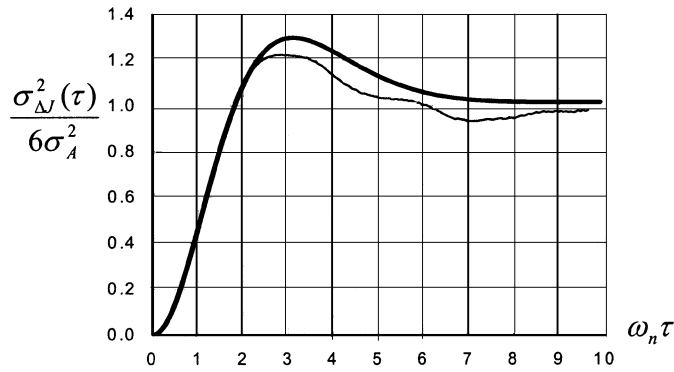


Fig. 8. Normalized adjacent-period-jitter variance caused by flicker frequency noise: theory (thick line) versus simulation (thin line).

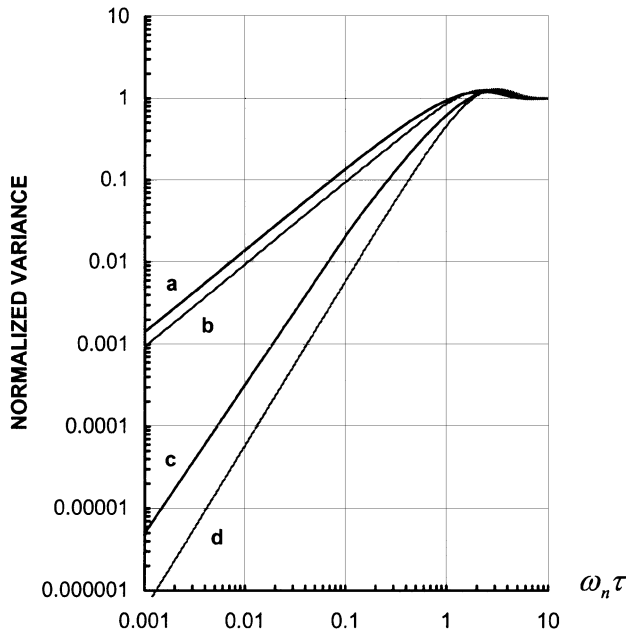


Fig. 9. Log-log plot of normalized variance versus  $\omega_n \tau$  for white frequency noise: (a) period jitter, and (b) adjacent period jitter; and for flicker frequency noise: (c) period jitter, and (d) adjacent period jitter.

variance on the measurement interval (curve “c”) is slower than quadratic. Recall that in Section III, it was indicated that  $\sigma_J^2(\tau)$  is not well defined for free-running oscillators with flicker frequency noise. Furthermore, the bound in (11d) of Section II indicates that for any process, doubling the measurement interval can at most quadruple the period-jitter variance. As a direct consequence of (10) and (16), the short-term period jitter variance over two related time scales (measurement intervals) has a quadratic dependence in the time scale (measurement interval)

$$4\sigma_J^2(\tau) - \sigma_J^2(2\tau) = 8 \ln(2) c_{FN} \tau^2. \quad (31)$$

In summary, increasing natural frequency  $\omega_n$  and reducing VCO jitter minimizes absolute jitter. The improvement in absolute jitter can be predicted using (27). Jitter variances scale linearly with  $c$  and  $c_{FN}$ , and the relative contribution of  $1/f$  noise to absolute jitter can be predicted using (28). When  $1/f$  noise and white noise contribute equally to absolute jitter (Fig. 9), white noise is the dominant cause of short-term (adjacent) period jitter for measurement intervals less than  $1/\omega_n$ . If  $1/f$  noise is a

factor of 40 (160) higher, the effect of white noise on (adjacent) period jitter is significant over measurement intervals shorter than  $0.01/\omega_n$ , with the contribution of flicker noise exceeding that of white noise over longer measurement intervals. The decision to reduce white noise or  $1/f$  noise contribution should depend on the interval over which (adjacent) period jitter is to be minimized.

## VII. MIXED-SIGNAL JITTER SIMULATION

In a PLL as depicted in Fig. 2, the VCO and the input stage of the feedback divider run at the highest frequency  $f_{OUT}$ , while clock pulses arrive at the input to the phase detector at a moderate rate  $f_{OUT}/N$ . Operating at the lowest frequency, the loop filter takes an average of the phase error over many cycles, and produces a correction signal for the VCO. Due to this multi-rate characteristic, achieving high simulation speed and timing accuracy, over long simulation intervals, is vital.

In this work, the entire PLL is simulated using ADVance MS. Digital blocks such as phase/frequency detector and frequency dividers are modeled using VHDL. Analog/mixed-signal components such as charge pump, loop filter and VCO are modeled using VHDL-AMS. Sampled-data characteristic and minimum pulse width in the PFD, together with mismatch in the charge pump, cause “reference” spurs in the VCO output (at  $f_{IN}/M$ ), and are modeled. Extra care ensures that the PFD model is well behaved when input pulses arrive at the same time. The effect of random mismatches in transistors can be predicted using efficient sensitivity calculations in a circuit simulator [19], without resorting to Monte Carlo simulations. The composite oscillator-divider model described in [3] uses a novel technique to simulate random jitter caused by white and flicker frequency noise, and is used in this work. This model preserves fundamental noise properties such as long-term memory and self-similarity in temporal- as well as spectral-domain. The same technique is used to model random jitter in the VCO and  $1/f$  jitter in the frequency dividers. In a basic model of a VCO, the phase is obtained by circular integration of the VCO frequency

$$\phi_{VCO}(t) = \int K_{VCO} v_C(t) dt \bmod 2\pi. \quad (32)$$

Special attention is given to minimizing jitter due to numerical noise. The above modulus operation causes discontinuities in the phase. Since the phase appears in the argument of a periodic function, this type of discontinuities is harmless and should be ignored by the continuous-time simulation kernel. Instinctively, VCO jitter is often simulated by dithering the frequency term. However, this causes random jumps in the time-derivative of the phase, and can degrade simulation accuracy and speed. Fast, smooth, and accurate simulation is achieved by dithering the modulus term.

A 2.56 GHz charge-pump PLL is simulated to validate the theoretical results presented in Sections II and VI. This PLL has feedback divider ratio of 16, VCO gain of 1 GHz/volt, and charge-pump current of 1.2 mA. The loop filter is designed so that the natural frequency of the PLL is  $8.7e6$  rad/s. Figs. 5 and 6 show the normalized period-jitter variance, due to VCO jitter caused by white and flicker frequency noise. Similarly, Figs. 7 and 8 show the normalized adjacent-period-jitter variance. Table I gives PLL jitter statistics for a measurement in-

TABLE I  
PLL JITTER STATISTICS

|                        | RMS jitter in ps<br>(Measurement interval $kT = 6.25$ ns) |            |                                     |            |
|------------------------|---|------------|-------------------------------------|------------|
|                        | White noise<br>$c = 1.6e-17$ s                            |            | Flicker noise<br>$c_{FN} = 1.6e-11$ |            |
|                        | Theory  | Simulation | Theory                              | Simulation |
| Absolute jitter        | 0.81  | 0.84       | 0.58                                | 0.62       |
| Period jitter          | 0.31  | 0.33       | 0.069                               | 0.074      |
| Adjacent period jitter | 0.45  | 0.47       | 0.059                               | 0.065      |

interval that corresponds to the sampling rate of the PFD. Simulation results and analytical predictions are within 10% of each other.

### VIII. EFFECT OF $1/f$ JITTER IN FREQUENCY DIVIDERS ON PLLS

Flicker noise in frequency dividers has an interesting, not previously known, effect on the behavior of first- and higher-order PLLs. Analysis of the PLL model in Fig. 3 shows that the transfer function from a divider output to the PLL output is given by

$$\frac{\phi_{OUT}}{\phi_{FD}} = \pm N H(s) \quad (33)$$

where  $H(s)$  is the low-pass filter in (21). Narrowing the loop bandwidth should reduce the effect of jitter in frequency dividers. However, suppose additive noise in a frequency divider causes absolute jitter with  $1/f$  spectrum. Assuming  $\phi_{FD}$  has the same spectrum,  $S\phi_{OUT}$  has  $1/f$  dependence at low frequencies, below the loop bandwidth. Consequently, input–output tracking jitter (the PLL output relative to the reference input) has a potentially unbounded variance. The variation in the skew between the two phase-detector inputs is the phase-detector error. The transfer function from a divider output to the phase-detector error is identical to the high-pass filter in (22), except for the sign

$$\frac{\phi_E}{\phi_{FD}} = \pm \{1 - H(s)\}. \quad (34)$$

The  $S\phi_E$  spectrum has  $1/f$  dependence above the loop bandwidth. With a finite upper frequency limit, absolute jitter in the phase-detector error has a bounded variance.

To verify these theoretical predictions,  $1/f$  jitter is added to the output of the reference divider. The charge-pump PLL of Section VII, with natural frequency of  $8.7e6$  rad/s and damping factor of 4, is simulated using ADVance MS. Fig. 10 shows  $S\phi(f)$  spectrum for both inputs to the PFD and the timing error between inputs to the PFD. The noisy divider (“a” in Fig. 10) operates at an output frequency of 160 MHz, and has output  $1/f$  noise of  $-141$  dB  $\text{rad}^2/\text{Hz}$  at 300 kHz, similar in performance to high-speed frequency dividers in [9] and [10]. The  $1/f$  spectrum is low-pass filtered by the PLL to produce the “b” spectrum at the output of the feedback divider (or equivalently, at

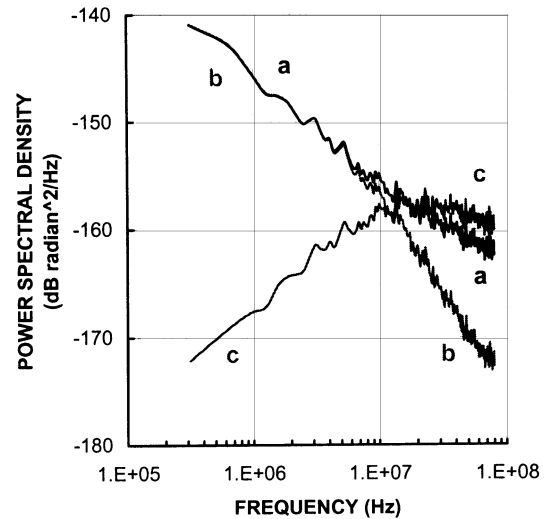


Fig. 10. Spectral density of absolute jitter at (a) reference input to phase detector, (b) feedback input to phase detector, and (c) phase-detector error, caused by  $1/f$  jitter in reference divider.

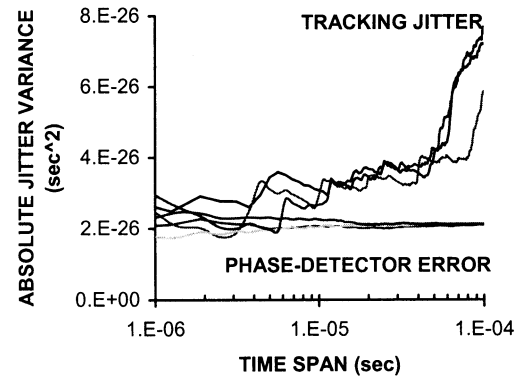


Fig. 11. Tracking jitter and phase-detector error, relative to nominal period of 6.25 ns, caused by  $1/f$  jitter in frequency divider, for three independent simulations.

the feedback input to the PFD). Because of  $1/f$  dependence at low frequencies, input–output tracking jitter is potentially unbounded. The timing error between inputs to the PFD (phase-detector error) has the “c” spectrum, and is bounded, as predicted. Delay in the feedback divider causes the “c” spectrum to rise nearly 2 dB higher than the  $1/f$  spectrum above the loop bandwidth. Fig. 11 gives the absolute jitter variance as a function of the time span for three independent simulations using three sets of random seeds. Comparing this result with Table I, jitter caused by divider noise is in the same order of magnitude as PLL jitter due to VCO noise. The figure clearly shows that while the phase-detector error is bounded, the input–output tracking jitter grows with time, as predicted. This should not be surprising, since a PLL is designed to follow slow variations in the inputs to the phase detector. The phase-detector error (or equivalently, the variation in the VCO control voltage) provides a false impression that the PLL output is in “phase-lock” with the reference input. On–off switching of MOS transistors can potentially reset long-term memory in  $1/f$  noise [20], [21] and lessen the problem, though it is not known if this novel technique is effective for all sources of  $1/f$  noise. It is worthwhile to note that if noises at both frequency dividers are correlated, some jitter cancellation can occur.

TABLE II  
MEASUREMENT-INTERVAL DEPENDENCE OF SHORT-TERM PERIOD JITTER AND  
ADJACENT PERIOD JITTER IN OSCILLATORS AND PLLS

| Dependence on measurement interval $\tau$ | White noise      |                         | Flicker noise             |                         | Equations and Figures |
|---|------------------|-------------------------|---------------------------|-------------------------|-----------------------|
|   | $\sigma_j(\tau)$ | $\sigma_{\Delta}(\tau)$ | $\sigma_j(\tau)$          | $\sigma_{\Delta}(\tau)$ |                       |
| Oscillators                               | Square root      |                         | Undefined                 | Linear                  | (16)-(17)             |
| First-order PLL                           | Square root      |                         | Absolute jitter unbounded |                         | (25)                  |
| Second-order PLL                          | Square root      |                         | Sub-linear                | Linear                  | (29)-(31), Fig. 9     |

## IX. CONCLUSION

Jitter in clock signals is minimized to achieve accurate analog-to-digital conversion in mixed-signal circuits, and establish reliable synchronization in data processing, networking and communication systems. Depending on the application, different measures of clock jitter are needed. Three time-domain measures of clock jitter were reviewed, and their intricate interdependencies uncovered, yielding a remarkably simple relation between period jitter and adjacent period jitter. These relations were used to analyze the effect of white noise and flicker noise on jitter in oscillators, as well as short-term and long-term jitter in phase-locked loops.

Analysis of jitter in free-running oscillators revealed that rms adjacent-period jitter, caused by  $1/f$  noise, grows linearly with the measurement interval, but surprisingly rms period jitter is not well-defined. In addition, rms (adjacent) period jitter, due to white noise, grows with the square root of the measurement interval.

Analysis of jitter in phase-locked loops revealed that short-term (adjacent) period jitter has the same measurement-interval dependence as jitter in a free-running VCO, provided both are defined (Table II). In first- and second-order PLLs, white frequency noise in the VCO causes short-term (adjacent) period jitter to grow with the square root of the measurement interval. In a first-order PLL, flicker frequency noise in the VCO causes absolute jitter to become potentially unbounded. In a second-order PLL, flicker frequency noise in the VCO causes short-term rms (adjacent) period jitter to grow at a sub-linear (linear) rate. These observations are summarized in Table II. Analysis also revealed that when noise in the reference divider or the feedback divider causes jitter with  $1/f$  spectrum, input-output tracking jitter in any PLL grows with time and is potentially unbounded. Techniques for achieving accurate and fast jitter simulations were described, and simulation results confirmed analytical predictions. Design implications for optimizing short-term and long-term PLL jitter, in the presence of white and  $1/f$  noise, were given.

## ACKNOWLEDGMENT

The author would like to thank P. Larsson, H. Wang, and R. Booth for fruitful discussions on phase-locked loops, and reviewers for invaluable comments. He would also like to thank A. Fakhfakh for pointing out an alternative definition of "cycle-to-cycle" jitter in [12].

## REFERENCES

- [1] T. C. Weigandt, B. Kim, and P. R. Gray, "Analysis of timing jitter in CMOS ring oscillators," in *Proc. Int. Symp. Circuits and Systems*, vol. 4, 1994, pp. 27–30.
- [2] A. Demir, A. Mehrotra, and J. Roychowdhury, "Phase noise in oscillators: A unifying theory and numerical methods for characterization," *IEEE Trans. Circuits Syst. I*, vol. 47, pp. 655–674, May 2000.
- [3] D. C. Lee, "Modeling of timing jitter in oscillators," in *Proc. Forum Design Languages*, Lyon, France, Sept. 3–7, 2001.
- [4] J. A. McNeill, "Jitter in ring oscillators," *IEEE J. Solid-State Circuits*, vol. 32, pp. 870–879, June 1997.
- [5] M. Mansuri and C. K. K. Yang, "Jitter optimization based on phase-locked loop design parameters," in *Proc. Int. Solid-State Circuits Conf. Dig. Tech. Papers*, 2002, pp. 138–139.
- [6] A. Hajimiri, S. Limotyrakis, and T. H. Lee, "Jitter and phase noise in ring oscillators," *IEEE J. Solid-State Circuits*, vol. 34, pp. 790–804, June 1999.
- [7] W. F. Egan, "Modeling phase noise in frequency dividers," *IEEE Trans. Ultrason., Ferroelect. Freq. Contr.*, vol. 37, no. 4, pp. 307–315, 1990.
- [8] M. R. McClure, "Residual phase noise of digital frequency dividers," *Microwave J.*, vol. 35, no. 3, pp. 124–130, 1992.
- [9] J. Craninckx and M. S. J. Steyaert, "A 1.75-GHz/3-V dual-modulus divide-by-128/129 prescaler in 0.7-um CMOS," *IEEE J. Solid-State Circuits*, vol. 31, pp. 890–897, July 1996.
- [10] N. Krishnapura and P. R. Kinget, "A 5.3-GHz programmable divider for HiPerLAN in 0.25-um CMOS," *IEEE J. Solid-State Circuits*, vol. 35, pp. 1019–1024, July 2000.
- [11] F. M. Gardner, *Phaselock Techniques*, 2nd ed. New York: Wiley, 1979.
- [12] F. Herzel and B. Razavi, "A study of oscillator jitter due to supply and substrate noise," *IEEE Trans. Circuits Syst. II*, vol. 46, pp. 56–62, Jan. 1999.
- [13] P. Larsson, "Measurements and analysis of PLL jitter caused by digital switching noise," *IEEE J. Solid-State Circuits*, vol. 36, pp. 1113–1119, July 2001.
- [14] R. H. Walden, "Analog-to-digital converter survey and analysis," *IEEE J. Select. Areas Commun.*, vol. 17, pp. 539–550, 1999.
- [15] A. Zanchi, A. Bonfanti, S. Levantino, and C. Samori, "General SSCR versus cycle-to-cycle jitter relationship with application to the phase noise in PLL," in *Proc. Southwest Symp. Mixed-Signal Design*, 2001, pp. 32–37.
- [16] J. Rutman and F. L. Walls, "Characterization of frequency stability in precision frequency sources," *Proc. IEEE*, vol. 79, pp. 952–960, June 1991.
- [17] A. Mehrotra, "Noise analysis of phase-locked loops," *IEEE Trans. Circuits Syst. II*, vol. 49, pp. 1309–1316, Sept. 2002.
- [18] K. Kishine, K. Ishii, and H. Ichino, "Loop-parameter optimization of a PLL for a low-jitter 2.5-Gb/s one-chip optical receiver IC with 1 : 8 DEMUX," *IEEE J. Solid-State Circuits*, vol. 37, pp. 38–50, Jan. 2002.
- [19] D. C. Lee, B. W. McNeill, K. Singhal, and K. Singhal, "Mismatch modeling and simulation of analog MOS circuits," Bell Labs Tech. Memo., 1996.
- [20] S. L. J. Gierkink, E. A. M. Klumperink, A. P. van der Wel, G. Hoogzaad, E. van Tuijl, and B. Nauta, "Intrinsic  $1/f$  device noise reduction and its effect on phase noise in CMOS ring oscillators," *IEEE J. Solid-State Circuits*, vol. 34, pp. 1022–1025, July 1999.
- [21] H. Tian and A. El Gamal, "Analysis of  $1/f$  noise in switched MOSFET circuits," *IEEE Trans. Circuits Syst. II*, vol. 48, Feb. 2001.



**David C. Lee** (M'92–SM'02) received the B.A.Sc. and M.A.Sc. degrees in systems design engineering from the University of Waterloo, Waterloo, ON, Canada, in 1986 and 1988, respectively.

From 1988 to 1989, he was a Process Engineer with Northern Telecom, Ottawa, ON, Canada. From 1989 to 1992, he was a Member of Scientific Staff with Bell Northern Research, Ottawa. From 1992 to 1998, he was a Member of Technical Staff with AT&T Bell Laboratories, Allentown, PA. From 1999 to 2002, he was a Scientist with Mentor Graphics Corporation, Allentown. His current interests include analysis and simulation of high-performance analog/RF circuits simulation, statistical design for manufacturability, and mixed-signal behavioral modeling.

Mr. Lee is a Member of the Society for Industrial and Applied Mathematics (SIAM).